

論文の内容の要旨

論文題目: Low Dimensional Electronic Behavior in Bi Anti-dot Thin Films

(Bi アンチドット薄膜における低次元電子状態に関する研究)

氏名: Park Youngok

(パク ヨンオク)

朴 瑛玉

Bismuth (Bi) nanostructures have attracted considerable attention due to its quantum confinement effect originating from small electron effective mass of about $0.001m_e$ and large spin-orbit interaction [1]: The small effective mass as well as low carrier density, which is 4-5 orders of magnitude smaller than those of typical metals [2], result in the unusual carrier transport properties of Bi, such as long Fermi wavelength (λ_F) of ~ 40 nm [3] and long carrier mean free path of ~ 100 nm at 300 K and ~ 400 μm at 4 K [4]. As the dimensionality of Bi nanostructures becomes lower, unique electric and thermal transport properties due to the quantum confinement effect appear, such as semimetal to semiconductor transition [5] and enhanced thermoelectric conversion efficiency [6], which have been indeed observed in Bi nanostructures whose dimensions are smaller than λ_F .

Numbers of studies have been devoted to fabrication of low dimensional Bi structures so far. However, it is still difficult not only to handle very thin films or single nanowires but also to measure their physical properties. Anti-dot structures with tailored pore neck lengths are suitable for investigating the correlation between dimensionality and electronic structure of Bi, because their dimensionality is much easier to control. In this study, I focused on anti-dot Bi thin films fabricated on anodized aluminium oxide template (AAO). The pore neck length (w) and film thickness (t) were systematically varied as experimental parameters that govern the dimensionality of the anti-dot structure. Based on the analysis of magneto-resistance (MR) as a function of external field, the dimensionality of the anti-dot Bi thin films was deduced. As a result, I found dimensional crossover from quasi-1D to 3D with increasing w and t .

Preparation of Bi anti-dot films

Aluminium (Al) thin films with 0.8-1 μm -thick were deposited on unheated $\alpha\text{-Al}_2\text{O}_3$ (0001) substrates by RF sputtering. A high purity Al target (99.999 %) was used. To obtain smooth Al films, it is needed to suppress the coalescence of neighboring grains during thin film growth due to unintentional substrate heating by plasma. Here I employed cycle deposition method, in which 90 nm-thick deposition and 30 minutes cooling were alternatively repeated in nine times cycles. The base pressure was maintained at 5×10^{-5} Pa. The working pressure was set to 3.25×10^{-1} Pa with 250 W deposition power under Ar gas of 5 sccm at room temperature.

The Al thin films thus prepared were subjected to two-step anodization [7] with 0.3 M oxalic acid solution under the constant voltage of 40 V at 4 $^\circ\text{C}$. After second anodization, the pore neck length w was controlled in a range of 30 nm - 60 nm by pore widening process with phosphoric acid solution. On the obtained anodized aluminium oxide (AAO) templates, Bi anti-dot structures were grown by thermal evaporation at 10^{-5} Pa at room temperature with a deposition rate of 0.17 nm/s. Bi thin films with three different thicknesses t , 25 nm, 35 nm and 50 nm, were prepared.

Surface structures of the AAO templates and Bi anti-dot films were probed by field-emission scanning electron microscope (SEM). Figures 1(a) and (b) are plain-view SEM images of AAO templates indicating hexagonal arrays of pores with averaged w of 30 nm and 60 nm, respectively. In the former, w is shorter than λ_F , ~ 40 nm, while longer in the latter. SEM images of the 25 nm-thick and 50 nm-thick Bi anti-dot films on the two AAO templates with different w are shown in Figs. 1(c)-(d) and Figs. 1(e)-(f), respectively. While all of the films kept anti-dot shape on the $w = 30$ nm templates, the anti-dot shape disappeared in the films thicker than 25 nm on the $w = 60$ nm templates due to lateral growth of Bi (Fig. 1(f)). X-ray diffraction measurements revealed that the anti-dot Bi films were in polycrystalline phase. Furthermore, no peaks from Al metal were detected, indicating that the Al films were completely oxidized during the anodization process.

Weak antilocalization effect and dimensional crossover in the Bi anti-dot films

In order to investigate the dimensionality of the obtained Bi anti-dot films, I focused on weak antilocalization (WAL) effect: In a disordered Bi system, the large spin-orbit interaction induces WAL effect, i.e., reduction of electrical resistance under conditions of low temperature and low magnetic field. Furthermore, the magnetic-field dependence of WAL effect reflects the dimensionality of the material, as discussed later on. Thus, magneto-transport properties of the films were characterized by four probe resistance down to 2 K under external magnetic field from 0 T to 9 T applied

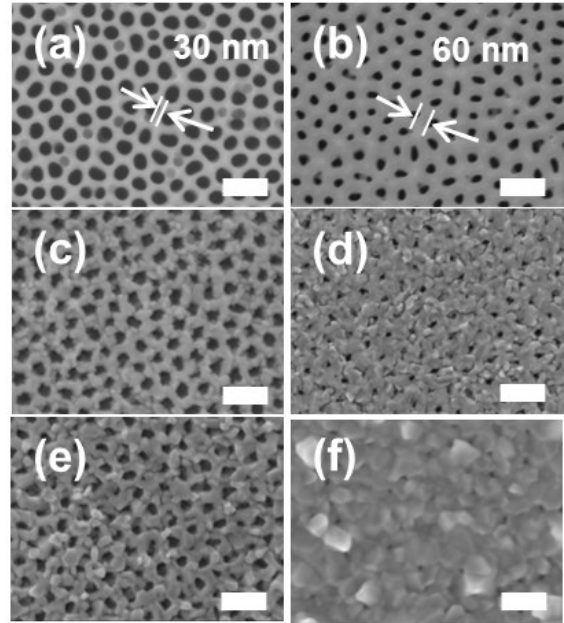


Fig 1. (a,b) Plain-view SEM images of AAO template ((a) $w = 30$ nm, (b) 60 nm). (c-f) SEM images of (c, d) $t = 25$ nm and (e, f) $t = 50$ nm Bi anti-dot films ((c, e) $w = 30$ nm, (d,

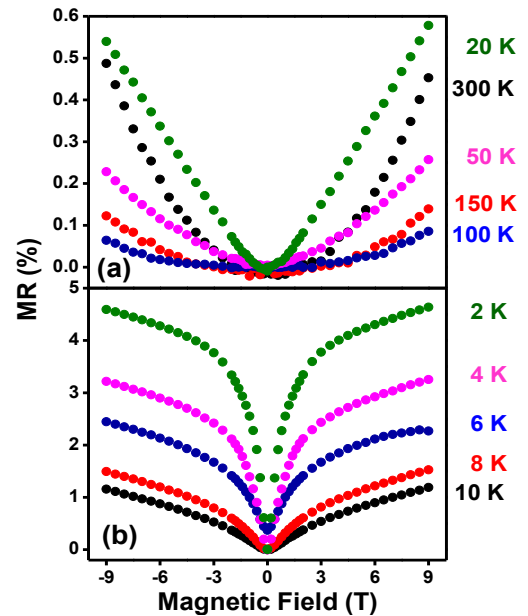


Fig 2. MR data for $w30/t25$ Bi anti-dot film at various temperatures ((a) 300

under conditions of low temperature and low magnetic field. Furthermore, the magnetic-field dependence of WAL effect reflects the dimensionality of the material, as discussed later on. Thus, magneto-transport properties of the films were characterized by four probe resistance down to 2 K under external magnetic field from 0 T to 9 T applied

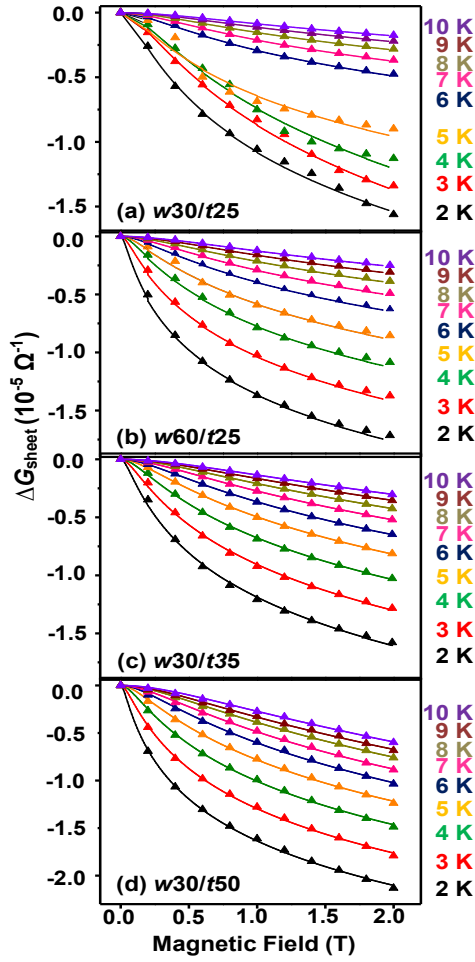


Fig 3. Magnetic field dependence of the sheet conductance of Bi anti-dot films deposited on AAO templates at various temperatures. (a) $w30/t25$, (b) $w60/t25$, (c) $w30/t35$, and (d) $w30/t50$.

dimensionality is reasonable because both t (25 nm) and w (30 nm) are shorter than λ_F of Bi, 40 nm. In case of $w60/t25$ (Fig. 4(b)) and $w30/t35$ (Fig. 4(c)), no dimensional crossovers were encountered, and the b values are in a range between 1/2 and 1, suggesting that they are in 2D regime at the whole temperature range of 2-10 K. $w30/t50$ is inferred to be 3D, from the fitting result in Fig. 4(d) ($b = 1$). These results indicate that the anti-dot films grown on AAO template indeed show low-dimensional transport properties when w or t becomes smaller than λ_F .

Summary

The dimensionalities of anti-dot Bi thin films were studied by adjusting two parameters, pore neck length w and film thickness t . I found that the Bi anti-dot structure systematically changed its electronic dimensionality from quasi-1D to 3D, depending on both parameters. In the film with thickness of 25 nm and pore neck distance of 30 nm, a quasi-1D feature was observed in the low temperature-low field regime, 2 K-6 K and 0 T-2 T, reflecting a fact that the coherence length is always longer than the two

perpendicular to the film surface.

Figure 2 displays the obtained magneto-resistance ($MR(\%) = 100[R(H, T) - R(0, T)]/R(0, T)$) vs filed (H) curves for the $t = 25$ nm Bi anti-dot film on $w = 30$ nm AAO template (hereafter referred to as $w30/t25$). The $MR-H$ curves drastically changed with respect to temperature. At high temperature ($T > 20$ K, Fig. 2(a)), MR shows parabolic like shape and does not saturate up to 9 T, as seen in classical MR. On the contrary, below 10 K, MR sharply decreases with decreasing H (Fig. 2(b)). This indicates that the film is out of the classical regime and that WAL effect becomes dominant. In addition, MR tends to be saturated at higher H . This behavior is also recognizable in the 35 nm-thick film ($w30/t35$) and 50 nm-thick film on $w=30$ nm templates ($w30/t50$) as well as 25 nm-thick one with $w= 60$ nm ($w60/t25$).

In two-dimensional localization theory based on Hikami-Larkin-Nagaoka (HLN) model [8], WAL effect can be described by the following expression.

$$\Delta G_{sheet}(H) = \alpha \frac{e^2}{2\pi^2 \hbar} \times \left[\psi \left(\frac{1}{2} + \frac{H_\phi}{H} \right) - \ln \left(\frac{H_\phi}{H} \right) \right], \quad (1)$$

where $\Delta G_{sheet}(H) = G_{sheet}(H) - G_{sheet}(0)$ is the quantum correction to the sheet conductance, α is a prefactor, ψ denotes the Digamma function, and $H_\phi = \hbar/4e\mu_0 L_\phi^2$ where L_ϕ is the coherence length. The ΔG_{sheet} vs H curves observed in the low temperature – low field region (0-2 T and 2-10 K) are depicted in Fig. 3, which show clear WAL effect. I carried out fitting of eq.(1) to the experimental $\Delta G_{sheet}(H)$ in Fig. 3, and plot the deduced L_ϕ values as functions of temperature (Fig. 4). Theoretically, L_ϕ is given by a power law function of T , as T^b , and the b parameter is a measure of the dimensionality: $b = 1/3$ for one-dimensional (1D), $b = 1/2$ for two-dimensional (2D) and $b = 1$ for three-dimensional (3D) systems. As seen from Fig. 4(a), the $\log L_\phi$ vs T plot of the $w30/t25$ film shows a clear inflection point at ~ 6 K, demonstrating a dimensional crossover. From 2 K to 6 K, the film is considered to be in between 1D and 2D (quasi-1D) with $b = 0.46$. Meanwhile, above 6 K, the b value increased to 0.83. This low

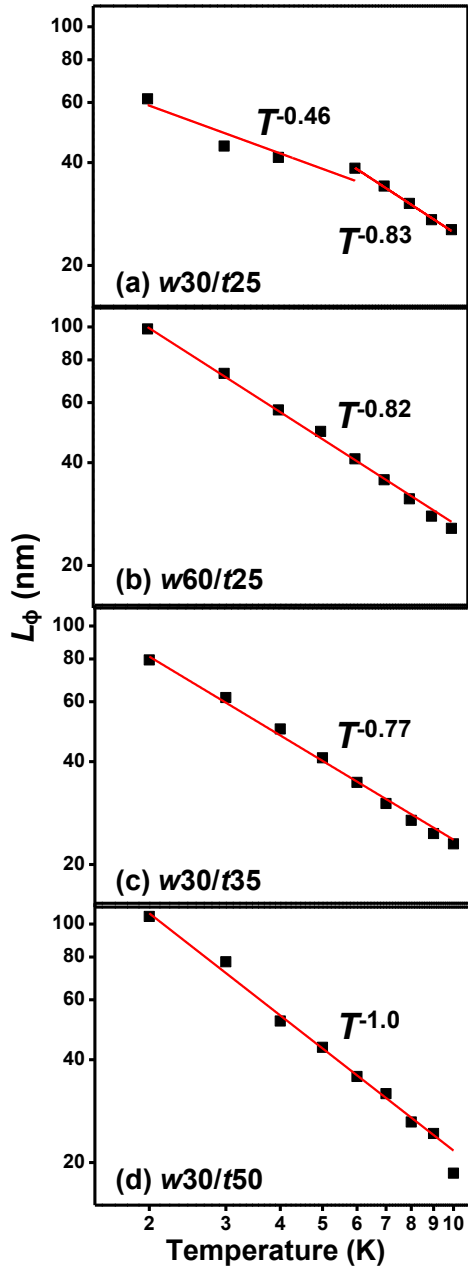


Fig 4. Temperature dependence of coherence length evaluated by fitting eq.(1) to the data in Fig. 3. The solid lines exhibit the results of

parameters. Meanwhile, in the cases that only w or t is smaller than the Fermi wavelength, the obtained Bi anti-dot films showed two dimensional behavior at 2 K-10 K. The film with both w and t longer than λ_F exhibited a 3D nature.

The quasi-1D behavior observed in the w_{30}/t_{25} film implies that nanowire-like behavior is induced by spatial restriction effect at pore necks. In order to realize clearer 1D behavior, fabrication of thinner Bi films with narrower pore neck length is a promising approach. The present Bi anti-dot system is quite useful for studying the low dimensional physical properties, because of not only the easiness in sample handling, but also an expectation for novel physical properties, such as enhanced thermoelectric effect, due to the unique low dimensional network structure.

References

- [1] J. Heremans, C. M. Thrush, Y. M. Lin, S. Cronin, Z. Zhang, M. S. Dresselhaus and J. F. Mansfield, Phys. Rev. B **61**, 2921 (2000).
- [2] G. E. Smith, J. M. Rowell, G. A. Baraff, Phys. Rev. A **135**, 1118 (1964).
- [3] J. H. Manges, J. P. Issi, J. Heremans, Phys. Rev. B **14**, 4381 (1976).
- [4] D. H. Reneker, Phys. Rev. Lett. **1**, 440 (1958).
- [5] S. Lee, J. Ham, K. Jeon, J. Noh and W. Lee, Nanotechnology **21**, 405701 (2010).
- [6] A. Boukai, K. Xu and J.R. Heath, Adv. Mater. **18**, 864 (2006).
- [7] H. Masuda and K. Fukuda, Science, **268**, 1466 (1995).
- [8] S. Hikami, A. I. Larkin and Y. Nagaoka, Prog. Theor. Phys. **63**, 707 (1980).